Environmental Science & Technology

pubs.acs.org/est

Article

Role of Iron Sulfide Phases in the Stability of Noncrystalline Tetravalent Uranium in Sediments

Luca Loreggian, Julian Sorwat, James M. Byrne, Andreas Kappler, and Rizlan Bernier-Latmani*

Cite This: *Environ. Sci. Technol.* 2020, 54, 4840–4846

Read Online

ACCESS | Metrics & More | Article Recommendations | Supporting Information

ABSTRACT: Uranium (U) *in situ* bioremediation has been investigated as a cost-effective strategy to tackle U contamination in the subsurface. While uraninite was believed to be the only product of bioreduction, numerous studies have revealed that noncrystalline U(IV) species (NCU(IV)) are dominant. This finding brings into question the effectiveness of bioremediation because NCU(IV) species are expected to be labile and susceptible to oxidation. Thus, understanding the stability of NCU(IV) in the environment is of crucial importance. Fe(II) minerals (such as FeS) are often associated with U(IV) in bioremediated or naturally reduced sediments. Their impact on the stability of NCU(IV) is not well understood. Here, we show that, at high dissolved oxygen concentrations, FeS accelerates NCU(IV) reoxidation. We hypothesize that either highly reactive ferric minerals or radical S species produced by the oxidation of FeS drive this rapid reoxidation of NCU(IV). Furthermore, we found evidence for the contribution of reactive oxygen species to NCU(IV) reoxidation. This work refines our understanding of the role of iron sulfide minerals in the stability of tetravalent uranium in the presence of oxygen in a field setting such as contaminated sites or uranium-bearing naturally reduced zones.

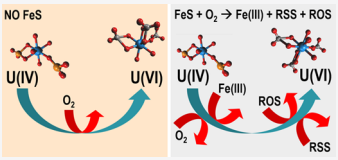

INTRODUCTION

Uranium (U) contamination in the subsurface is a concern in former and present uranium mining, milling, and processing sites. When an elevated concentration of U is found in aquifers, health risks may require remediation. U mobility depends on its speciation and redox state with reducing species being, in general, relatively insoluble and immobile. Thus, reduction of U(VI) to U(IV), either through biological activity[1] or abiotic processes,[2] results in the net immobilization of U. In recent years, the stimulation of microbial activity, leading to U immobilization (bioremediation), has drawn significant interest, and it has been recognized as a potentially cost-effective alternative[3] to more invasive remediation techniques, such as excavation.

However, while uraninite (UO_2, a crystalline tetravalent uranium oxide) was initially believed to be the dominant species of bioreduced U(IV), laboratory and field studies have revealed that noncrystalline tetravalent species (NCU(IV)) prevail after biotic reduction[4−6] and in naturally reduced zones.[7,8] Relative to UO_2, NCU(IV) appears to be more sensitive to reoxidation by oxygen[9−11] and to form soluble U(IV) carbonate complexes more readily.[12] The effectiveness of bioremediation is dependent on the resistance of U(IV) to reoxidation. Therefore, it is crucial to understand the stability of NCU(IV) in the environment and its resistance to reoxidation and remobilization upon contact with O_2-bearing water. The reduced U could come into contact with oxygen as a result of the seepage of rainfall through the soil or the seasonal change in the water table level, exposing the reduced zone to atmospheric O_2.

The sediment that has undergone bioremediation typically harbors reduced minerals such as Fe(II)-bearing minerals. In sulfur-containing systems, iron sulfide phases (such as mackinawite, FeS) are often found in association with U.[5,13] The presence of such reduced phases was hypothesized to provide a redox buffer, consuming O_2 and resulting in the retardation of U(IV) oxidation. Indeed, this redox-protective effect was demonstrated in laboratory experiments in which FeS was reacted with UO_2 in the presence of O_2.[11] However, the impact of FeS appears to depend greatly on the speciation of U(IV). A similar experiment considering NCU(IV) instead of UO_2 was carried out and evidenced the enhanced oxidative dissolution of U(IV) by FeS under oxic conditions via an undefined oxidative pathway.[10] The production of highly reactive Fe(III) species was proposed as a mechanism for FeS-enhanced NCU(IV) oxidation.[10] The abovementioned work was conducted in simple mixtures of synthetic FeS and either synthetic UO_2 or biologically produced NCU(IV), amended with O_2. Thus, the role of FeS in the oxidation of U(IV) by O_2 remains ill-defined in environmentally relevant conditions that include complex mixtures of minerals and the presence of microorganisms.

Finally, reactive oxygen species (ROS) represent chemically reactive species that contain oxygen and are produced through a variety of mechanisms, including in the absence of light.[14−16] ROS have been proposed as strong oxidants for metals that

Received: November 26, 2019
Revised: March 6, 2020
Accepted: March 13, 2020
Published: March 13, 2020

https://dx.doi.org/10.1021/acs.est.9b07186
Environ. Sci. Technol. 2020, 54, 4840–4846

naturally occur in the subsurface, such as iron,[14,17] copper,[18] manganese,[19] and arsenic.[20] The presence of ROS has been evidenced in a shallow uranium-contaminated groundwater at the Old Rifle site (CO, USA), particularly at the oxic−anoxic interface,[21] making them potentially relevant for the investigation of U(IV) oxidation in aquifers.

This work aims to investigate the impact of FeS on the oxygen-dependent oxidation of NCU(IV) in sediments and to explore whether ROS production contributes to NCU(IV) oxidation and remobilization. To do so, sediments from the Old Rifle site (CO, USA) were biostimulated with anoxic artificial groundwater amended with U and multiple electron donors under (i) sulfate-reducing conditions to favor the formation of FeS and (ii) iron-reducing conditions as a control system lacking FeS. The oxygen-mediated oxidation of NCU(IV) that accumulated in these sediments was tested under batch and flow-through conditions using artificial groundwater with a composition mimicking the aquifer at Old Rifle.

MATERIALS AND METHODS

Sediments. The sediment used in this study was collected in the background area of a former U milling processing site in Rifle (CO, USA) and stored in the dark until use. It is known in the literature as the Rifle area background sediment (RABS).[22−24] Columns were packed with RABS and biostimulated using artificial groundwater (Rifle artificial groundwater; GW) (Table S1) amended with a mixture of electron donors (i.e., molasses, glycerol, and yeast extract) and uranyl acetate to favor the precipitation of NCU(IV). The bioreduction phase in columns continued with incrementally higher U concentrations until an amount of U(IV) sufficient for spectroscopic investigation was accumulated in the sediments. More details about the design and operation of the columns are provided in a separate publication.[25] Two distinct influents were used for these columns: the first was Rifle artificial GW, which includes high sulfate (14 mM) to promote the proliferation of sulfate-reducing bacteria producing sulfide and thus establishing sulfate-reducing conditions (SRC); the second was a modified Rifle artificial GW lacking sulfate. Hence, in the latter case, bioavailable Fe(III), which naturally occurs in RABS at a concentration of ∼7 μmol/g,[23] was the primary electron acceptor and iron-reducing conditions (IRC) were established within the column. The IRC column thus was designed to provide sediments serving as a control to investigate the role of iron sulfides species during the reoxidation of NCU(IV).

Batch Oxidation Experiments. Batch experiments were performed using 3 g/L SRC or IRC sediments with oxic and suboxic Rifle artificial GW amended with 10 mM $NaHCO_3$ (final concentration) in glass bottles that were hermetically sealed with a butyl rubber stopper and an aluminum crimp and incubated under shaking conditions. The bottles had a total volume of 240 mL and the suspension represented a volume of 30 mL. Experiments were run in triplicate, but entire bottles were sacrificed at specific time points (3, 6, and 15 h) for characterization of the U solid phase. Prior to being used in these experiments, SRC and IRC sediments were washed with anoxic 50 mM $NaHCO_3$ to remove unreacted U(VI) adsorbed onto the solids. GW contained dissolved oxygen (DO) at a concentration of 8.56 mg/L and an oxic (21% O_2 by volume) headspace for experiments under oxic conditions and 2.14 mg/L and a suboxic headspace (5% O_2) for experiments under suboxic conditions. The suspensions of GW and sediments were continuously shaken in the dark, and the supernatant was routinely sampled and filtered through a 0.22 μm PTFE filter (Thermo Fisher, USA) for quantification of total dissolved U. Furthermore, to assess the contribution of ROS to U(IV) reoxidation, ROS production was quenched by the addition of 50 kU/L superoxide dismutase (SOD) and 100 kU/L catalase (CAT) (Sigma-Aldrich, USA) in control experiments.[15] This combination of enzymes rapidly degrades ROS due to the disproportionation of superoxide (HO_2) into water and peroxide by superoxide dismutase and the decomposition of H_2O_2 into H_2O and O_2 by catalase. To counter CAT instability and degradation, 150 μL of aliquots of CAT stock solution (200kU/L) was added to GW every 2 h for the entire duration of the experiment. At the end of the experiment, solid samples were collected for sediment characterization.

Flow-Through Oxidation Experiments. Oxic and suboxic flow-through oxidation experiments were conducted in custom-built Plexiglas continuously stirred tank reactors (CSTR) (volume of 12.5 mL) with no gas phase and an influent composed of Rifle artificial GW or Rifle artificial GW amended with 10 mM $NaHCO_3$ (final concentration). The sediment was maintained in the reactor by a 0.22 μm PTFE filter at the effluent end of the CSTR. Oxic experiments were run in triplicate, but an entire reactor was sacrificed at each specific time point (i.e., 21, 68, and 296 h). Suboxic experiments were run in duplicate. The influent was stored in a Tedlar bag to avoid gas exchange with the atmosphere and to maintain constant pH, DO, and bicarbonate concentration for the duration of the experiments. The suboxic experiments were conducted inside an anaerobic chamber (Coy Laboratory Products Inc., USA) with an atmosphere of 3%:97% H_2:N_2, but the influent DO content was carefully controlled. Each reactor was loaded with 1 g of SRC or IRC sediment, thus giving a solid-to-liquid ratio of 80 g/L. The flow rate was maintained between 0.9 and 1.1 mL/h by a peristaltic pump (Ismatec IP, Switzerland) and gravimetrically monitored during sampling. The resulting hydraulic residence time was ∼12.5 h. The entire effluent volume from the CSTRs was continuously collected. The pH values were occasionally measured in the effluents to ensure that they remained stable through the entire duration of the experiments. At 21 or 68 h and at the end of the experiment, an entire reactor was sacrificed to collect the solid samples for sediment characterization.

Wet Chemistry. Samples from batch and flow-through experiments were filtered through a 0.22 μm PTFE filter (ThermoFisher, USA), diluted and preserved in 0.1 M HNO_3 at 4 °C until analysis. Total dissolved uranium and sulfur (S) were determined by inductively coupled plasma mass spectrometry (ICP-MS; PerkinElmer ELAN DRC II) and inductively coupled plasma optical emission spectrometry (ICP-OES; Multitype ICP emission spectrometer, ICPE-9000, Shimadzu), respectively. The content of hydrogen peroxide (H_2O_2) was quantified in the effluent using a chemiluminescent method with acridinium ester, as shown by Cooper *et al.*[26] H_2O_2 is the most stable ROS, and its net production is typically interpreted as evidence for the presence of ROS;[21] a detailed description of the method is presented in the Supporting Information.

Sediment Characterization. Pristine RABS, bioreduced RABS prior to oxidation (i.e., SRC and IRC sediments), and oxidized sediments from select experiments were measured

https://dx.doi.org/10.1021/acs.est.9b07186
Environ. Sci. Technol. 2020, 54, 4840−4846

Table 1. Comparison of Relative Proportion of Iron Species in the Pristine Sediments before Bioreduction (RABS) and after Reduction (SRC and IRC), According to Mössbauer and Iron K-edge LCF EXAFS[a]

		(%)		(%)		(%)	
		Mössbauer*	EXAFS	Mössbauer	EXAFS	Mössbauer	EXAFS
model compound		RABS		SRC		IRC	
Fe in clays	Fe(II)_clays	28	45 ± 2	22 ± 7	71 ± 5	25 ± 0.3	59 ± 2
	Fe(III)_clays	28		5 ± 12		21 ± 0.3	
mackinawite	$Fe^{(II)}S$		*2 ± 2*	4 ± 16	25 ± 2		
	FeS_x			40 ± 13			
Fe in oxides	goethite	28	53 ± 3	13 ± 14	*4 ± 4*	18 ± 0.2	38 ± 3
	$hematite_{AF}$	9		16 ± 13		12 ± 0.2	
	$hematite_{WF}$					24 ± 0.1	
	magnetite	7					
	siderite						*2 ± 1*
χ^2/*R*-factor			0.015	0.6142	0.021	0.6988	0.016

[a]$Fe^{(II)}S$, potentially mackinawite; FeS_x, undefined Fe and S containing phase, potentially mackinawite; $hematite_{AF}$, hematite (antiferromagnetic); $hematite_{WF}$, weakly ferromagnetic. χ^2, reduced chi square (goodness of fit). Hyperfine parameters obtained by fitting Mössbauer data are reported in Table S9 and Figure S4; *, data reported from Komlos *et al.*[15] Numbers presented in italics are below the 10% operational cutoff expected to represent a detectable contribution for XAS. The full EXAFS dataset is presented in Table S15 and the reference spectra in Figure S8.

using X-ray absorption spectroscopy (XAS) at the U L_{III}-edge, the Fe K-edge and the S K-edge, and Mössbauer spectroscopy for Fe speciation and characterized by chemical extraction following a modified version of the method of Alessi *et al.*[12] for U speciation. Detailed descriptions of the techniques are presented in the Supporting Information.

RESULTS AND DISCUSSION

U, Fe, and S Speciation in Bioreduced Sediments. The bioreduced sediments, one produced under sulfate-reducing conditions (SRC) and the other under iron-reducing conditions (IRC), were characterized using chemical extraction and XAS. Regardless of the biogeochemical conditions, we report that the biostimulation of RABS results in the formation of NCU(IV) as the dominant product both in SRC and IRC sediments (Table S2). The dominant occurrence of NCU(IV) in SRC and IRC was confirmed by the solid-phase speciation of U in the two sediments using L_{III} X-ray near edge spectroscopy (XANES) LCF (Table S3 and Figure S1) and the extended X-ray absorption fine structure (EXAFS) shell-by-shell fit (Table S4 and Figure S2). The detailed modeling of the shell-by-shell fit is discussed in the Supporting Information. The two sediment types exhibit U speciation that is indistinguishable by XAS with >90% NCU(IV) and shell-by-shell fits that invoke the same components and similar coordination environments (Table S4).

In contrast, IRC, and SRC sediments exhibit distinct Fe speciation (Table 1). While the reduction of RABS in the presence of sulfate generates iron sulfide phases in the likely form of mackinawite, there is no detectable contribution from iron sulfides in IRC. Furthermore, iron oxides represent a greater contribution to total iron in IRC than in SRC sediments. This determination was made using a combination of Fe K-edge EXAFS and Mössbauer spectroscopy (Table 1). While EXAFS and Mössbauer provide clear evidence for the occurrence of FeS, there is a discrepancy in the quantification of the relative contributions of FeS and the other Fe phases in SRC. For instance, Mössbauer identified the presence of an FeS_x phase, which has been previously described as a poorly defined metastable phase that does not correspond to either FeS-, FeS_2-, or Fe_3S_4-type species.[27,28] This phase could not be identified using EXAFS; however, that is potentially due to the absence of an appropriate FeS_x reference. In contrast, the quantification of the Fe phases for IRC and pristine sediments are in good agreement within the uncertainties of each method. An exhaustive description of the Fe speciation in RABS, SRC, and IRC is provided in the Supporting Information. Thus, the results of the characterization of iron speciation in SRC and IRC underscore our hypothesis and what had been previously reported:[5,29] FeS forms upon bioreduction of RABS. In addition, we were able to verify that the control sediment, IRC, did not harbor detectable amounts of FeS. Due to their difference in Fe and S speciation, SRC and IRC also have distinct total electron equivalents contents: SRC contains 316 μmol total electron equivalent that results from the sum of total Fe(II) (68 μmol) and S(−II) (31 μmol), while IRC contains 26 μmol Fe(II), corresponding to only 26 μmol total electron equivalent. These calculations do not include the role of a natural organic matter, which surely contributes to the total electron equivalents. Overall, this dataset indicates that the speciation of U accumulating in the sediments during the bioreduction phase is independent from the biological reduction mechanism (i.e., sulfate vs iron reduction) and thus from the final speciation of iron in the sediment. The major difference in Fe speciation between these two conditions sets the stage for an investigation of the role of FeS in NCU(IV) oxidation by O_2 in sediment.

Batch Sediment Oxidation. The next step of the investigation was to compare the O_2-mediated oxidation of uranium in SRC and IRC sediments and probe whether the presence of FeS could impact the rate of U(IV) oxidation. Results show that, regardless of the type of sediment (i.e., SRC or IRC), U is released into solution upon exposure to oxygen where, under batch conditions, it accumulates (Figure 1). U is released more rapidly from SRC than IRC, both under oxic and suboxic conditions. As it was shown that SRC includes iron sulfide while IRC does not, we hypothesized that NCU(IV) reoxidation was faster when FeS occurred in bioreduced sediments exposed to O_2. This is consistent with the work of Bi *et al.*,[10] who observed an increase in the rate of oxidation of NCU(IV) in the presence of synthetic FeS. This finding is further supported by U speciation in the solid phase, which shows that, under oxic conditions, NCU(IV) is consumed more rapidly in SRC with only 75 ± 29 nmol out

https://dx.doi.org/10.1021/acs.est.9b07186
Environ. Sci. Technol. 2020, 54, 4840−4846

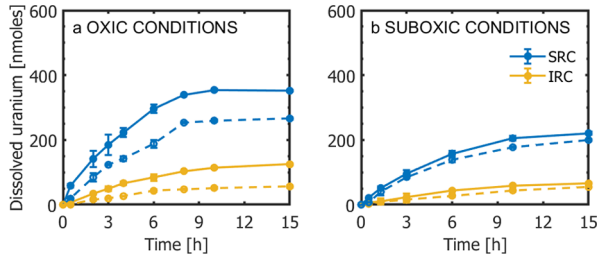

Figure 1. Uranium aqueous content over time during exposure to oxygen in a batch reactor for SRC and IRC sediments with and without SOD and CAT under (a) oxic and (b) suboxic conditions. Solid lines represent the experiment with no amendment, and dotted lines represent the amendment of SOD and CAT.

of the initial 459 ± 26 nmol remaining after 3 h of oxidation and only negligible amount of NCU(IV) remaining after 15 h (Figure 2a and Table S5), while in IRC, 210 ± 31 nmol (of the initial 368 ± 23 nmol) remain after 3 h and 100 ± 25 nmol remain after 15 h (Figure 2b and Table S6). As expected, the oxidation rate of NCU(IV) is lower under suboxic conditions than oxic conditions for both SRC and IRC sediments (Figure 2c,d and Tables S7 and S8). By comparison, we show that the contribution of recalcitrant U(IV), presumed to be UO_2, does not change during the entire duration of the oxidation experiment for all conditions (Figure 2). Thus, it is quite clear that NCU(IV) is the labile form of U(IV) and is the most susceptible to reoxidation in the presence of O_2.

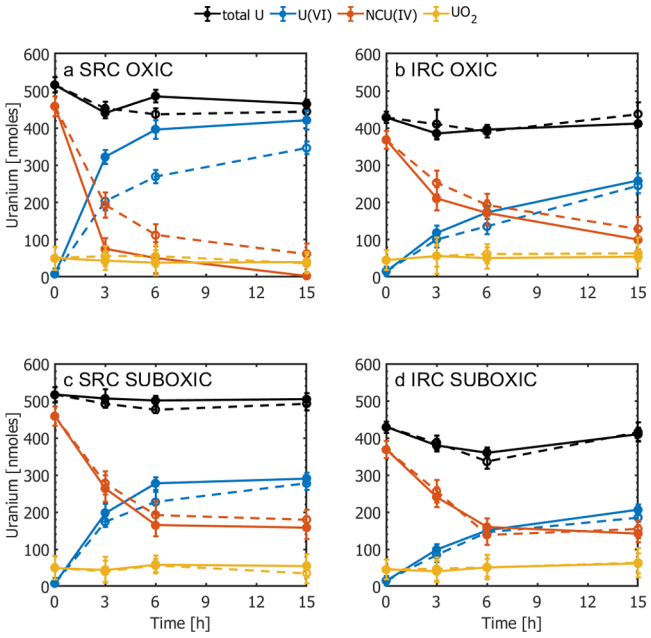

Figure 2. U speciation for sediments suspension (including soluble U) over time during the batch oxidation experiment under oxic conditions for (a) SRC and (b) IRC sediments and under suboxic conditions for (c) SRC and (d) IRC sediments. Solid lines represent the experiment with no amendment, and dotted lines represent the amendment of SOD and CAT. Blue represents aqueous and solid-associated U(VI), black represents total U, yellow represents UO_2, and orange represents NCU(IV). Data reported are results from the chemical extraction method modified from Alessi *et al.* The fraction of U(VI) is calculated as the sum of solution and solid-associated U(VI). Data for this figure are available in Tables S5 to S8.

At the same time, as U(IV) is oxidized, we observe the rapid oxidation of S species using S K-edge XANES (Table 2 and Figure S3). After 3 h of incubation, FeS, which represented 91 ± *1*% of S in SRC is no longer detectable with a concomitant increase in elemental sulfur (0) (from 1 ± *1* to 61 ± *2*%), sulfate (+VI) (from 3 ± *1* to 13 ± *1*%), and organic S(−I) (from 5 ± *1* to 27 ± *1*%) (Table 2). The rapid consumption of FeS in SRC is also confirmed by Mössbauer, which could not detect any evidence for the presence of FeS after 3 h of oxidation (Table S9 and Figure S4).

Table 2. LCF of S K-Edge XANES of SRC Sediments before and after Oxidation in Batch Experiments under Oxic Conditions[a]

	oxic			
model compound	initial (SRC)(%)	3 h(%)	6 h(%)	15 h(%)
mackinawite	91 ± 1			
elemental sulfur	*1* ± *1*	61 ± 2	58 ± 1	53 ± 1
S in organics	*5* ± *1*	27 ± 1	32 ± 2	35 ± 2
sulfate	*3* ± *1*	13 ± 1	10 ± 1	11 ± 1
R-factor	0.018	0.041	0.024	0.009

[a]The uncertainties of the fit are given in parenthesis for the last significant figure. The data are presented in Figure S3a and the references in Figure S9. Numbers presented in italics are below the 10% operational cutoff expected to represent a detectable contribution for XAS.

The oxidation of FeS by O_2 at neutral pH has been reported to occur via two processes: nonoxidative dissolution releasing Fe(II) and HS^- followed by homogeneous oxidation or surface mediation oxidation. Both processes ultimately form $Fe(OH)_3$, S^0, and SO_4^{2-}.[30] Consistent with these processes, we observe the formation of S^0 (Table 2) and an increase in the contribution of hematite and goethite by Mössbauer (Table S9) upon the oxidation of SRC sediments.

In contrast, the oxidation of IRC does not result in as extensive a shift in the overall Fe speciation. The main observation is a redistribution of Fe(III) among the existing pools of hematite (antiferromagnetic and weakly ferromagnetic) and goethite (Table S9). Surprisingly, we also observe an increase in the relative abundance of solid-phase Fe(II).

We observe that the reduction of NCU(IV) is accelerated by the oxidation of FeS and propose that a highly reactive $Fe(OH)_3$ phase could be produced that, in turn, oxidizes NCU(IV). Furthermore, the aerobic oxidation of sulfide generates intermediate valence sulfur species, including polysulfides, thiosulfate, and sulfite (SO_3^{2-}).[31] Among these, SO_3^{2-} represents a reactive species that is capable of oxidizing a range of transition metals (Fe(II), Mn(II), Ni(II), and Co(II)[32−35]) through a series of reaction steps that generate a number of strongly oxidizing radicals (i.e., $SO_3^{\bullet}$, $SO_5^{\bullet-}$, $SO_4^{\bullet-}$, and $HO^{\bullet}$).[36] Thus, we propose that the oxidation of FeS by oxygen generates species (whether Fe(III) or S bearing) that are highly reactive and that could contribute to the rapid oxidation of NCU(IV). Although reactive Fe(III) species are likely to form also in IRC, there is more Fe in SRC. Therefore, we expect that a larger pool of oxidants is generated upon exposure to oxygen, and these are responsible, along with reactive sulfur species, for the enhanced oxidation and remobilization of NCU(IV) in SRC.

Because the initial amount of U is not the same for SRC and IRC, it is not meaningful to compare percent NCU(IV)

https://dx.doi.org/10.1021/acs.est.9b07186
Environ. Sci. Technol. 2020, 54, 4840−4846

oxidized for the two conditions. Instead, we calculate that, after 15 h, 455 nmol NCU(IV) were consumed for SRC (Table S5) and 268 nmol for IRC (Table S6). Thus, ∼40% less amount of NCU(IV) was oxidized in IRC than in SRC under oxic conditions.

Similarly, we observe that 300 nmol NCU(IV) were oxidized in SRC under suboxic batch conditions (at 15 h), but only 226 nmol were oxidized in IRC (Tables S7 and S8). Thus, comparing the amount of NCU(IV) consumed, we calculate that 25% less NCU(IV) is oxidized in IRC as compared to SRC in the suboxic setting. This suggests that the greater the dissolved oxygen (DO) concentration, the more the presence of FeS accelerates NCU(IV) oxidation, or conversely, the lower the DO concentration, the smaller the difference in NCU(IV) oxidation rate between SRC and IRC.

Role of ROS. Peroxide is a ROS, and because it is the most readily measurable, it is often taken as an indicator of overall ROS production. Fieldwork at the Rifle site has demonstrated the presence of peroxide, particularly at the oxic−anoxic interface, suggesting a potential role for O_2 interaction with reduced species in the production of ROS.[21] Given that the system being studied here represents the oxic−anoxic interface, peroxide concentrations were probed upon exposure of SRC and IRC to oxygen. A net production of H_2O_2 was detected and interpreted as evidence for the generation of ROS (Figure S5). While it is out of the scope of this work to unravel the mechanism of ROS production in these systems, we observe that DO concentration and mineralogy both affect ROS production under the conditions investigated (Figure 1). ROS have been shown to oxidize reduced transition metals.[19,37] Thus, to gauge the potential role of ROS in NCU(IV) oxidation, we compare quenched experiments (i.e., those where SOD and CAT were added to quench ROS production) with unamended experiments (Figure 1). We observe that the rate of release of U and the amount of aqueous U were systematically lower in the quenched sediments than in the untreated sediments under oxic conditions for both SRC and IRC (Figure 1a). This finding indicates that the presence of ROS affects the rate of U(IV) oxidation and the mobilization of U(VI) into the aqueous phase. The change in the extent of oxidation may reflect the depletion of the substrate for ROS formation (perhaps Fe(II)). Further, we consider the solid-phase speciation as a function of time (Figure 2a,b), and we interpret the difference in the number of moles of NCU(IV) remaining after 15 h of oxidation in the systems with and without SOD/CAT as the total contribution of ROS to U(IV) reoxidation. We report that ROS contributes to 13 and 8% of the total oxidation of NCU(IV) in SRC and IRC under oxic conditions, respectively (Table S10). Furthermore, as the production of ROS depends on the DO concentration (Figure S5), we expected that their contribution to U(IV) reoxidation is greater under oxic conditions than under suboxic conditions. Indeed, we report that the contribution of ROS in SRC and IRC decreases to 5 and 3%, respectively, under suboxic conditions (Figures 1 and 2 and Table S10).

We have demonstrated that ROS contribute to the reoxidation of NCU(IV) with a more significant contribution when the DO concentration is higher. However, a comparison of the rate of NCU(IV) oxidation in SRC and IRC in the presence of SOD and CAT (Figure 2) also evidences the fact that, even in the absence of ROS, NCU(IV) is still oxidized more rapidly in SRC than in IRC. This is evidenced by comparing the dotted lines in Figure 2a,b, representing the SOD- and CAT-reacted SRC (Figure 2a) and IRC (Figure 2b) sediments and showing more rapid oxidation in the former case. Thus, we conclude that, while the reaction with ROS is a contributing mechanism to the overall oxidation of NCU(IV), it cannot entirely account for the differences between the rates of NCU(IV) oxidation in SRC and IRC sediments.

Flow-Through Sediment Oxidation. When SRC is oxidized in flow-through reactors at a low flow rate (i.e., 0.8 m/d as at the Old Rifle site), U(IV) oxidation (followed by U mobilization to the aqueous phase) as well as the oxidation of the reduced species of Fe and S in the solid phase proceed at a slower rate than in batch systems. Indeed, in the SRC sediment, a 7% contribution of FeS remains after 21 h of oxidation based on S K-edge XANES (Table S11 and Figure S3b) and 8% based on Fe K-edge EXAFS (Table S14 and Figure S6); when in the batch system, no FeS remained after 3 h (Table 2 and Figure S3a) and only 68% of NCU(IV) was oxidized after 21 h in the CSTR (Table S12) when ∼83% was oxidized after 3 h in the batch system (Table S5).

Moreover, the differences between the SRC and IRC system are much more muted (practically nonexistent) under flow-through than under batch conditions but still show slightly faster release of aqueous U in the presence of FeS than in its absence, particularly from ∼70 to 200 h (Figure 3). We attribute this muted effect to the specific experimental conditions. Indeed, while the headspace of the batch system, containing excess O_2, constantly equilibrates with the aqueous phase, establishing a steady DO concentration throughout the entire period of the experiment, the influx of DO in the flow-through reactor is controlled by the flow rate (i.e., 8.56 μgO_2/

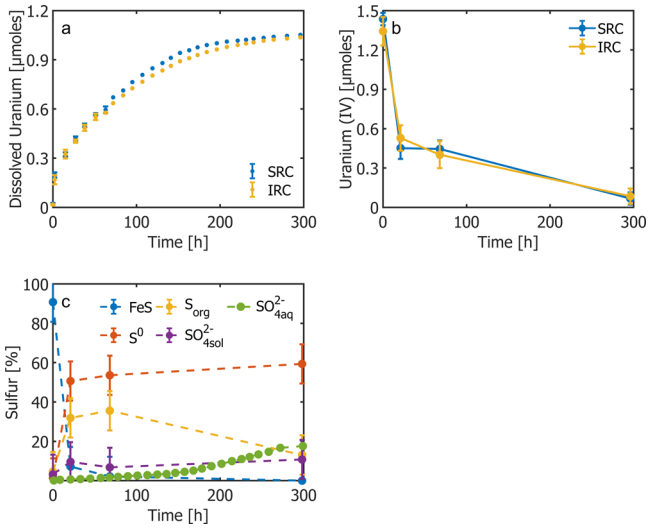

Figure 3. Oxidation of SRC and IRC sediments under oxic conditions in the flow-through system in the presence of 10 mM bicarbonate. (a) Cumulative uranium released over time with SRC (blue markers) and IRC (yellow markers) sediments under oxic conditions. (b) Solid-phase NCU(IV) concentration over time in SRC (blue markers) and IRC (yellow markers). Data reported in panel (b) are results from the chemical extraction method modified from Alessi *et al.* (c) Sulfur speciation expressed as a percentage based on the initial S content (determined by XRF), on S K-edge LCF XANES speciation, and SO_4^{2-} measured in solution ($SO_4^{2-}{}_{aq}$) (Figure S11) and in the solid phase (SO4 2-sol). Note that the percent contribution of each species does not reflect the values in Table 2 because of the contribution from the aqueous phase.

https://dx.doi.org/10.1021/acs.est.9b07186
Environ. Sci. Technol. 2020, 54, 4840−4846

h). In essence, DO is a limiting factor in the flow-through system, whereas it is not in the batch system. We hypothesize that the formation of highly reactive iron oxide minerals or sulfur species may be oxygen-limited in the flow-through system, resulting in a lesser impact of FeS on U(VI) oxidation.

Continuing along the same line as earlier with the batch experiments, we estimate that 0.99 μmol NCU(IV) are oxidized at 21 h for SRC and 0.81 μmol for IRC. Thus, we calculate the ratio of the amount of NCU(IV) oxidized at 21 h for IRC to that for SRC in the oxic CSTR experiment (Table S12). In this case, we obtain a value of 82%. Furthermore, the suboxic flow-through experiment exhibits a ratio of the amount of NCU(IV) oxidized in IRC relative to that in SRC of 88% after 296 h (Table S13 and Figure S7).

Thus, as the availability of DO decreases (in the order oxic batch > suboxic batch > oxic flow-through > suboxic flow-through), the ratio of the initial rate of NCU(IV) oxidation in IRC to that in SRC increases (59, 75, 82, and 88%). This trend suggests that the oxidation of FeS impacts the oxidation of NCU(IV) in a DO-dependent manner. Thus, at high DO values, FeS oxidation by O_2 will have the greatest impact on NCU(IV) oxidation.

Overall, we confirm the results obtained in the previous study that was based on pure NCU(IV) and synthetic FeS.[10] We conclude that FeS oxidation accelerates the oxidation of NCU(IV) in sediments either via the formation of reactive ferric minerals or sulfur-bearing radicals in an oxygen-dependent manner and through an unknown mechanism. Additionally, there is no evidence that FeS can provide a redox buffer, actually slowing the rate of oxidation of NCU(IV), as it appears to occur with UO_2.[11]

Environmental Implications. FeS has primarily been investigated for its capacity to reduce contaminants in the environment. Indeed, iron sulfide phases are ubiquitous and an essential part of the biogeochemical cycle of Fe and S. Furthermore, during *in situ* bioreduction, when sulfate-reducing conditions are established, FeS rapidly immobilizes U(VI), and it is commonly reported in association with U(IV). The overall picture that emerges from considering the role of FeS in oxidative processes in this study is that FeS can also significantly accelerate the oxidation of NCU(IV) in oxygen-rich locations. We hypothesize that this enhanced rate of NCU(IV) reoxidation may involve transient reactive S species or highly reactive ferric oxide phases. To a lesser extent, ROS will play a role in NCU(IV) oxidation, depending on the amount of O_2 available in the system.

The conditions that favor a role for FeS in U(IV) oxidation are a high amount of oxygen and abundant FeS in proximity to U(IV) hotspots. Thus, an ideal scenario would be one in which there is a significant influx of O_2 into a low-permeability, anoxic sediment where sulfate-reducing conditions prevail. Because oxidation of NCU(IV) is likely catalyzed by solid phases (i.e., Fe(III) and perhaps S^0) as well as, to a lesser extent, reactive oxygen species, the relative localization of U and Fe is of critical importance.

We expect that such conditions are unlikely to be observed in a site such as Old Rifle. Even though conditions are favorable for the formation of FeS and to the colocalization of U and FeS, the characteristics of the aquifer (i.e., slow groundwater velocity and low permeability) limit oxygen diffusion, which is the essential condition triggering the cascade of reactions forming reactive species that oxidize U(IV). Therefore, while the conditions investigated in this study represent an extreme scenario at Rifle, it may be more relevant in sites characterized by coarser-grained sediments such as the sites of Grand Junction or Naturita (Colorado, USA) where conditions are also favorable for the formation of iron sulfides species and O_2 is rapidly transported through the sediments.

■ ASSOCIATED CONTENT

Supporting Information

The Supporting Information is available free of charge at https://pubs.acs.org/doi/10.1021/acs.est.9b07186.

Additional data (PDF)

■ AUTHOR INFORMATION

Corresponding Author

Rizlan Bernier-Latmani − *Environmental Microbiology Laboratory (EML), EPFL-ENAC-IIE-EML, Ecole Polytechnique Federale de Lausanne (EPFL), Lausanne CH-1015, Switzerland;* orcid.org/0000-0001-6547-722X; Email: rizlan.bernier-latmani@epfl.ch

Authors

Luca Loreggian − *Environmental Microbiology Laboratory (EML), EPFL-ENAC-IIE-EML, Ecole Polytechnique Federale de Lausanne (EPFL), Lausanne CH-1015, Switzerland;* orcid.org/0000-0001-7509-6551

Julian Sorwat − *Center for Applied Geoscience (ZAG), Eberhard Karls Universitaet Tuebingen, Tuebingen 72076, Germany*

James M. Byrne − *Center for Applied Geoscience (ZAG), Eberhard Karls Universitaet Tuebingen, Tuebingen 72076, Germany;* orcid.org/0000-0002-4399-7336

Andreas Kappler − *Center for Applied Geoscience (ZAG), Eberhard Karls Universitaet Tuebingen, Tuebingen 72076, Germany;* orcid.org/0000-0002-3558-9500

Complete contact information is available at: https://pubs.acs.org/10.1021/acs.est.9b07186

Notes

The authors declare no competing financial interest.

■ ACKNOWLEDGMENTS

This study is funded by the Swiss National Science Foundation under grant #200020-144335. The S K-edge and Fe K-edge XAS experiments were performed on the 4-3 and 4-1 beamline at the Stanford Synchrotron Radiation Lightsource (SSRL). We are grateful for the technical assistance received during the XAS analyses from Ryan Davis, Erik Nelson, and Matthew Latimer. The use of the SSRL, SLAC National Accelerator Laboratory is supported by the U.S. Department of Energy Office of Science, Office of Basic Energy Sciences under contract DE-AC02-76SF00515. We thank Vincent Noel for sharing the mackinawite model compounds for the XAS analysis of S and Fe data. We thank Manon Frutschi for the help and support in the lab.

■ REFERENCES

(1) Lovley, D. R.; Phillips, E. J. P.; Gorby, Y. A.; Landa, E. R. Microbial Reduction of Uranium. *Nature* **1991**, *350*, 413.

(2) Veeramani, H.; Alessi, D. S.; Suvorova, E. I.; Lezama-Pacheco, J. S.; Stubbs, J. E.; Sharp, J. O.; Dippon, U.; Kappler, A.; Bargar, J. R.; Bernier-Latmani, R. Products of Abiotic U(VI) Reduction by Biogenic Magnetite and Vivianite. *Geochim. Cosmochim. Acta* **2011**, *75*, 2512−2528.

(3) Williams, K. H.; Bargar, J. R.; Lloyd, J. R.; Lovley, D. R. Bioremediation of Uranium-Contaminated Groundwater: A Systems Approach to Subsurface Biogeochemistry. *Curr. Opin. Biotechnol.* **2013**, *24*, 489−497.
(4) Bernier-Latmani, R.; Veeramani, H.; Vecchia, E. D.; Junier, P.; Lezama-Pacheco, J. S.; Suvorova, E. I.; Sharp, J. O.; Wigginton, N. S.; Bargar, J. R. Non-Uraninite Products of Microbial U(VI) Reduction. *Environ. Sci. Technol.* **2010**, *44*, 9456−9462.
(5) Bargar, J. R.; Williams, K. H.; Campbell, K. M.; Long, P. E.; Stubbs, J. E.; Suvorova, E. I.; Lezama-Pacheco, J. S.; Alessi, D. S.; Stylo, M.; Webb, S. M.; Davis, J. A.; Giammar, D. E.; Blue, L. Y.; Bernier-Latmani, R. Uranium Redox Transition Pathways in Acetate-Amended Sediments. *Proc. Natl. Acad. Sci. U. S. A.* **2013**, *110*, 4506−4511.
(6) Alessi, D. S.; Lezama-Pacheco, J. S.; Janot, N.; Suvorova, E. I.; Cerrato, J. M.; Giammar, D. E.; Davis, J. A.; Fox, P. M.; Williams, K. H.; Long, P. E.; Handley, K. M.; Bernier-latmani, R.; Bargar, J. R. Speciation and Reactivity of Uranium Products Formed during in Situ Bioremediation in a Shallow Alluvial Aquifer. *Environ. Sci. Technol.* **2014**, *48*, 12842−12850.
(7) Bhattacharyya, A.; Campbell, K. M.; Kelly, S. D.; Roebbert, Y.; Weyer, S.; Bernier-Latmani, R.; Borch, T. Biogenic Non-Crystalline $U^{(IV)}$ Revealed as Major Component in Uranium Ore Deposits. *Nat. Commun.* **2017**, *8*, 15538.
(8) Noël, V.; Boye, K.; Lezama Pacheco, J. S.; Bone, S. E.; Janot, N.; Cardarelli, E.; Williams, K. H.; Bargar, J. R. Redox Controls over the Stability of U(IV) in Floodplains of the Upper Colorado River Basin. *Environ. Sci. Technol.* **2017**, *51*, 10954−10964.
(9) Cerrato, J. M.; Ashner, M. N.; Alessi, D. S.; Lezama-Pacheco, J. S.; Bernier-Latmani, R.; Bargar, J. R.; Giammar, D. E. Relative Reactivity of Biogenic and Chemogenic Uraninite and Biogenic Noncrystalline U(IV). *Environ. Sci. Technol.* **2013**, *47*, 9756−9763.
(10) Bi, Y.; Stylo, M.; Bernier-Latmani, R.; Hayes, K. F. Rapid Mobilization of Noncrystalline U(IV) Coupled with FeS Oxidation. *Environ. Sci. Technol.* **2016**, *50*, 1403−1411.
(11) Bi, Y.; Hayes, K. F. Surface Passivation Limited UO2 Oxidative Dissolution in the Presence of FeS. *Environ. Sci. Technol.* **2014**, *48*, 13402−13411.
(12) Alessi, D. S.; Uster, B.; Veeramani, H.; Suvorova, E. I.; Lezama-Pacheco, J. S.; Stubbs, J. E.; Bargar, J. R.; Bernier-Latmani, R. Quantitative Separation of Monomeric U(IV) from UO2 in Products of U(VI) Reduction. *Environ. Sci. Technol.* **2012**, *46*, 6150−6157.
(13) Noël, V.; Boye, K.; Kukkadapu, R. K.; Bone, S.; Lezama Pacheco, J. S.; Cardarelli, E.; Janot, N.; Fendorf, S.; Williams, K. H.; Bargar, J. R. Understanding Controls on Redox Processes in Floodplain Sediments of the Upper Colorado River Basin. *Sci. Total Environ.* **2017**, *603-604*, 663−675.
(14) Page, S. E.; Kling, G. W.; Sander, M.; Harrold, K. H.; Logan, J. R.; McNeill, K.; Cory, R. M. Dark Formation of Hydroxyl Radical in Arctic Soil and Surface Waters. *Environ. Sci. Technol.* **2013**, *47*, 12860−12867.
(15) Zhang, T.; Hansel, C. M.; Voelker, B. M.; Lamborg, C. H. Extensive Dark Biological Production of Reactive Oxygen Species in Brackish and Freshwater Ponds. *Environ. Sci. Technol.* **2016**, *50*, 2983−2993.
(16) Vermilyea, A. W.; Dixon, T. C.; Voelker, B. M. Use of $H_2{}^{18}O_2$ To Measure Absolute Rates of Dark H_2O_2 Production in Freshwater Systems. *Environ. Sci. Technol.* **2010**, *44*, 3066−3072.
(17) Voelker, B. M.; Sulzberger, B. Effects of Fulvic Acid on Fe(II) Oxidation by Hydrogen Peroxide. *Environ. Sci. Technol.* **1996**, *30*, 1106−1114.
(18) Pham, A. N.; Xing, G.; Miller, C. J.; Waite, T. D. Fenton-like Copper Redox Chemistry Revisited: Hydrogen Peroxide and Superoxide Mediation of Copper-Catalyzed Oxidant Production. *J. Catal.* **2013**, *301*, 54−64.
(19) Learman, D. R.; Voelker, B. M.; Vazquez-Rodriguez, A. I.; Hansel, C. M. Formation of Manganese Oxides by Bacterially Generated Superoxide. *Nat. Geosci.* **2011**, *4*, 95−98.
(20) Tong, M.; Yuan, S.; Ma, S.; Jin, M.; Liu, D.; Cheng, D.; Liu, X.; Gan, Y.; Wang, Y. Production of Abundant Hydroxyl Radicals from Oxygenation of Subsurface Sediments. *Environ. Sci. Technol.* **2016**, *50*, 214−221.
(21) Yuan, X.; Nico, P. S.; Huang, X.; Liu, T.; Ulrich, C.; Williams, K. H.; Davis, J. A. Production of Hydrogen Peroxide in Groundwater at Rifle, Colorado. *Environ. Sci. Technol.* **2017**, *51*, 7881−7891.
(22) Anderson, R. T.; Vrionis, H. A.; Ortiz-Bernad, I.; Resch, C. T.; Long, P. E.; Dayvault, R.; Karp, K.; Marutzky, S.; Metzler, D. R.; Peacock, A.; White, D. C.; Lowe, M.; Lovley, D. R. Stimulating the In Situ Activity of Geobacter Species To Remove Uranium from the Groundwater of a Uranium-Contaminated Aquifer. *Appl. Environ. Microbiol.* **2003**, *69*, 5884−5891.
(23) Komlos, J.; Peacock, A.; Kukkadapu, R. K.; Jaffé, P. R. Long-Term Dynamics of Uranium Reduction/Reoxidation under Low Sulfate Conditions. *Geochim. Cosmochim. Acta* **2008**, *72*, 3603−3615.
(24) Moon, H. S.; Komlos, J.; Jaffé, P. R. Uranium Reoxidation in Previously Bioreduced Sediment by Dissolved Oxygen and Nitrate. *Environ. Sci. Technol.* **2007**, *41*, 4587−4592.
(25) Loreggian, L.; Novotny, A.; Bretagne, S. L.; Bartova, B.; Wang, Y.; Bernier-Latmani, R. The Effect of Aging on the Stability of Microbially-Reduced Uranium in Natural Sediments. *Environ. Sci. Technol.* **2020**, 613.
(26) Cooper, W. J.; Moegling, J. K.; Kieber, R. J.; Kiddle, J. J. A Chemiluminescence Method for the Analysis of H2O2 in Natural Waters. *Mar. Chem.* **2000**, *70*, 191−200.
(27) Thiel, J.; Byrne, J. M.; Kappler, A.; Schink, B.; Pester, M. Pyrite Formation from FeS and H2S Is Mediated through Microbial Redox Activity. *Proc. Natl. Acad. Sci. U. S. A.* **2019**, *116*, 6897−6902.
(28) Wan, M.; Schröder, C.; Peiffer, S. Fe(III):S(-II) Concentration Ratio Controls the Pathway and the Kinetics of Pyrite Formation during Sulfidation of Ferric Hydroxides. *Geochim. Cosmochim. Acta* **2017**, *217*, 334−348.
(29) Moon, H. S.; McGuinness, L.; Kukkadapu, R. K.; Peacock, A. D.; Komlos, J.; Kerkhof, L. J.; Long, P. E.; Jaffé, P. R. Microbial Reduction of Uranium under Iron- and Sulfate-Reducing Conditions: Effect of Amended Goethite on Microbial Community Composition and Dynamics. *Water Res.* **2010**, *44*, 4015−4028.
(30) Jeong, H. Y.; Han, Y.-S.; Park, S. W.; Hayes, K. F. Aerobic Oxidation of Mackinawite (FeS) and Its Environmental Implication for Arsenic Mobilization. *Geochim. Cosmochim. Acta* **2010**, *74*, 3182−3198.
(31) Kumar, N.; Pacheco, J. L.; Noël, V.; Dublet, G.; Brown, G. E., Jr. Sulfidation Mechanisms of Fe(III)-(Oxyhydr)Oxide Nanoparticles: A Spectroscopic Study. *Environ. Sci.: Nano* **2018**, *5*, 1012−1026.
(32) Berglund, J.; Fronaeus, S.; Elding, L. I. Kinetics and Mechanism for Manganese-Catalyzed Oxidation of Sulfur(IV) by Oxygen in Aqueous Solution. *Inorg. Chem.* **1993**, *32*, 4527−4538.
(33) Coichev, N.; van Eldik, R. A Fascinating Demonstration of Sulfite Induced Redox Cycling of Metal Ions Initiated by Shaking. *J. Chem. Educ.* **1994**, *71*, 767.
(34) Warneck, P.; Ziajka, J. Reaction Mechanism of the Iron(III)-Catalyzed Autoxidation of Bisulfite in Aqueous Solution: Steady State Description for Benzene as Radical Scavenger. *Bunsen-Ges. Phys. Chem., Ber.* **1995**, *99*, 59−65.
(35) Muller, J. G.; Hickerson, R. P.; Perez, R. J.; Burrows, C. J. DNA Damage from Sulfite Autoxidation Catalyzed by a Nickel(II) Peptide. *J. Am. Chem. Soc.* **1997**, *119*, 1501−1506.
(36) Dong, H.; Chen, J.; Feng, L.; Zhang, W.; Guan, X.; Strathmann, T. J. Degradation of Organic Contaminants through Activating Bisulfite by Cerium(IV): A Sulfate Radical-Predominant Oxidation Process. *Chem. Eng. J.* **2019**, *357*, 328−336.
(37) Nico, P. S.; Anastasio, C.; Zasoski, R. J. Rapid Photo-Oxidation of Mn(II) Mediated by Humic Substances. *Geochim. Cosmochim. Acta* **2002**, *66*, 4047−4056.

https://dx.doi.org/10.1021/acs.est.9b07186
Environ. Sci. Technol. 2020, 54, 4840−4846